# Inconspicuous structural coloration in the elytra of beetles *Chlorophila obscuripennis* (Coleoptera)

Feng Liu, Haiwei Yin, Biqin Dong, Youhua Qing, Li Zhao, Serge Meyer, and Xiaohan Liu*
*Surface Physics Laboratory and Department of Physics, Fudan University, Shanghai 200433, People's Republic of China*

Jian Zi†
*Surface Physics Laboratory and Department of Physics, Fudan University, Shanghai 200433, People's Republic of China and T-Life Research Centre, Fudan University, Shanghai 200433, People's Republic of China*

Bin Chen
*College of Life Sciences, Chongqing Normal University, Shapingba, Chongqing 400047, People's Republic of China*
(Received 31 October 2007; published 17 January 2008)

The elytra of male beetles *Chlorophila obscuripennis* (Coleoptera) display an inconspicuous iridescent bluish green color. By structural characterizations we find that the outermost elytral surface comprises a sculpted multilayer, which is the origin of structural coloration. In elytra both structural green and cyan colors are observed which arise from the modulations imposed on the multilayer, leading to a bluish green color by color mixing. The adoption of the sculpted multilayer can render structural coloration inconspicuous, which could be advantageous for camouflage. In addition, it can cause light emergence at nonspecular angles.

DOI: 10.1103/PhysRevE.77.012901 PACS number(s): 42.66.−p, 42.25.−p, 87.19.−j

## I. INTRODUCTION

Structural colors result from the interactions of natural light with featured microstructures comparable to visible wavelengths [1–7]. They are widespread in the biological world, found in insects [8–16], birds [17–26], sea animals [27–29], and even in plants [30–33]. The studies of structural colors and their structural origin may render important information on their functionalities such as signal communications, conspecific recognition, camouflage, etc. Besides, the revealed structures may inspire not only the designs of optical structures but also the way of their engineering [34].

In this paper, we study the structural and optical properties of the elytra of beetle *Chlorophila obscuripennis* (Coleoptera) by optical microscope, scanning electron microscopy (SEM), transmission electron microscopy (TEM), and reflectance measurements. Beetle *Chlorophila obscuripennis* belongs to a small family of *Lagriidae* (long-jointed beetles), which can be often found in eastern Tibet and Wolong District (famous for the panda), Sichuan Province, China. The male displays an inconspicuous iridescent bluish green color in elytra. Our aim is to uncover the origin of structural coloration in elytra and to investigate the optical effects of the revealed microstructures.

This paper is organized as follows. Section II presents optical microscope, SEM, and TEM images of the elytra of beetle *Chlorophila obscuripennis*, which provide us with the microstructures responsible for the observed iridescence and their structural parameters. Specular and nonspecular reflectance measurements are given in Secs. III and IV, respectively. Section V contains discussions.

## II. STRUCTURAL CHARACTERIZATIONS

The specimens used for our studies were obtained from Shanghai Natural Museum, Shanghai, China. Structural characterizations were done by optical microscope, SEM, and TEM. The optical microscope image of an elytron is shown in Fig. 1. When viewed with the naked eye, elytra show an inconspicuous iridescent bluish green color. With the oblique observation, it changes to an inconspicuous blue. Under the high magnification, the iridescent bluish green color is actually additive mixtures of a green color in the framework of hexagonal veins and a cyan color in the center. The remaining part shows a rather dull blue color which gives a minor contribution to color mixing.

The microstructures of elytra were characterized by both SEM and TEM, shown in Figs. 2 and 3, respectively. From the top view we can see that the outer surface of an elytron is not flat. Instead, it comprises an array of hexagonal pits. Compared with the optical microscopic images, there exists an exact correspondence between the surface morphology and the observed color pattern: the pit ridges produce a green color, the basins a cyan color, and the inclined sides a dull blue color. All these colors change with viewing angle. The pits measure about 11 $\mu$m across and 2.8 $\mu$m in depth. The transverse cross-section images reveal that the outermost cuticle consists of a sculpted multilayer which conforms to the elytral surface morphology.

From TEM images we can determine the structural parameters of the sculpted multilayer. It is composed of about

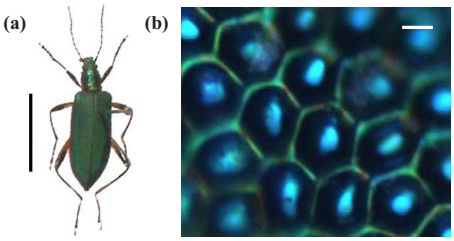


FIG. 1. (Color online) (a) Optical image of a male beetle *Chlorophila obscuripennis*. Its elytra display an inconspicuous iridescent bluish green color. (b) Optical microscopic image of an elytron under 1000× magnification. Scale bars, (a) 1 cm and (b) 5 $\mu$m.

*liuxh@fudan.edu.cn
†jzi@fudan.edu.cn

 

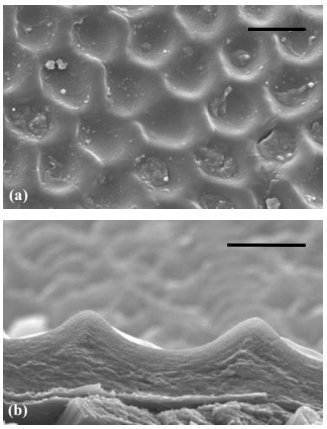


FIG. 2. SEM images of elytra. (a) Top view of the outer elytral surface. The elytral surface comprises of an array of hexagonal pits. (b) Transverse cross section of the outermost elytra surface. Scale bars, (a) 10 $\mu$m and (b) 5 $\mu$m.

16 thin layers with alternating low and high electron density, which are the source of the elytral structural coloration. The layer with low electron density is chitin. By chemical treatments [9] we determined that the layer with high electron density may be melanoprotein. The average thickness of both chitin and melanoprotein layers shows distinct differences in different regions. The average thickness of the chitin layer is about 90, 85, and 78 nm at the ridge, the inclined side, and the basin, respectively. For the melanoprotein layer its average thickness in different regions is nearly the same, about 66 nm.

## III. SPECULAR REFLECTION

The specular reflection spectra of elytra at difference incident angles were measured by an optical spectrometer,

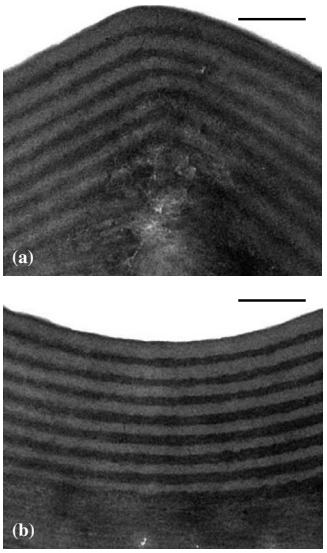


FIG. 3. TEM transverse cross section of (a) the ridge and (b) basin regions of the outermost elytra. Scale bars, 0.5 $\mu$m.

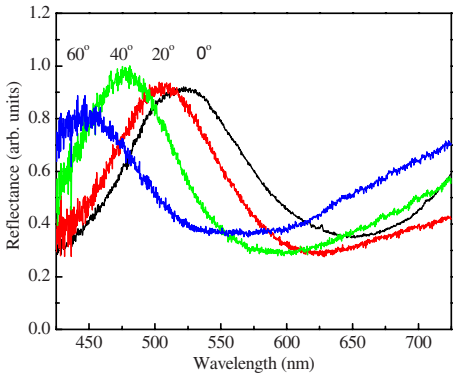


FIG. 4. (Color online) Normalized specular reflectance spectra of elytra at different incident angles.

shown in Fig. 4. At normal incidence, elytra exhibit a distinct reflection peak positioned at 520 nm, which is responsible for the bluish green color perceived by the naked eye. With increasing incident angle, this reflection peak undergoes a blueshift in wavelength: the peak position becomes 506, 477, and 446 nm at the incident angle of 20, 40, and 60 degrees, respectively. This corresponds to the observed iridescence. At large incident angles, the elytral color changes to blue.

As shown in the previous section, the outer surface of elytra comprises an array of hexagonal pits. The observed specular reflection comes dominantly from the regions that are perpendicular to the elytral surface normal, namely, the ridges and basins. The contribution from multiple reflections should be very small since the pit dimension is much larger than visible wavelengths. In other words, the observed reflection peak is a superposition of reflections from both the ridge and basin regions, eventually leading to a mixed color.

## IV. NONSPECULAR REFLECTION

The regions that are perpendicular to the elytral surface normal give rise to specular reflection. Nonspecular reflection is expected since the elytral surface is uneven. Specifically, the inclined sides of pits can produce nonspecular reflection. As a result, for a fixed incident angle, we cannot only observe specular reflection from the ridges and basins, but also nonspecular reflection from the inclined sides.

Figure 5 shows the measured reflection spectra for an elytron at normal incidence as a function of wavelength and emergence angle. At normal incidence, specular reflection occurs at zero emergence angle with a peak reflection positioned at about 520 nm. Obviously, a nonspecular reflection band can be seen. The intensity of nonspecular reflection is smaller than that of specular reflection. For normal incidence, nonspecular reflection occurs mainly at emergence angles that are smaller than 20°. Nonspecular reflection decreases with increasing emergence angle. At small emergence angles, nonspecular is dominant at about 520 nm, but it is dominant at shorter wavelength at large emergence angles.

## V. DISCUSSIONS

The outermost surface of elytra comprises a sculpted multilayer. This multilayer gives rise to structural coloration

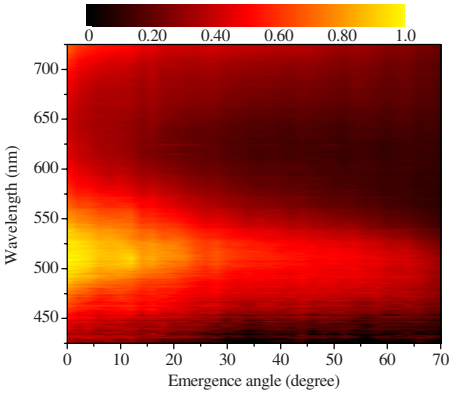


FIG. 5. (Color online) Relative emergence intensity as a function of wavelength and emergence angle at normal incidence in the color-scale form. The emergence angle is defined as the angle of reflected light with respect to the elytral surface normal.

and iridescence due to thin-film interference [35]. For a flat multilayer with alternating refractive indices, the wavelength of peak reflectance is given by

$$\lambda_{\max} = 2(n_1 d_1 \cos\theta_1 + n_2 d_2 \cos\theta_2), \quad (1)$$

where $n$ is the refractive index, $d$ is the layer thickness, and $\theta$ is the angle of refraction. The subscripts represent the layer index. The angle of refraction at different layers $\theta_1$ and $\theta_2$ can be obtained from Snell's law

$$n_1 \sin\theta_1 = n_2 \sin\theta_2 = \sin\theta_0, \quad (2)$$

where $\theta_0$ is the incident angle from air.

With the layer thickness parameters given in Sec. II, we can determine the wavelength peak reflectance. A refractive index of 1.56 is assumed for chitin, taken from Ref. [11], and the melanoprotein layer has a refractive index of 2.0, taken from Ref. [1]. In the ridge region the estimated wavelength of peak reflection at normal incidence is 545 nm, leading to a green color, which is consistent with the observation from the optical microscope. The estimated wavelength of peak reflection in the basin region is 507 nm at normal incidence, corresponding to a cyan color. The mixing of the two colors produces the perceived bluish green coloration.

As shown in Fig. 4, elytra display distinct iridescence which can be easily understood from Eq. (1). With increasing incident angle, the wavelength of peak reflection from both the ridge and basin regions undergoes a blueshift in wavelength. At the incident angle of 30°, the predicted wavelength of peak reflection from the ridge and basin becomes 522 and 486 nm, respectively, leading to blue coloration. The wavelength of peak reflection from the ridge and basin is shifted, respectively, to 472 and 440 nm at the incident angle of 60°. At large incident angles, the wavelength of peak reflection from the basin resides in violet.

Structural coloration in many beetles takes advantage of a flat multilayer [6,7]. However, the elytra of beetle *Chlorophila obscuripennis* possess a sculpted multilayer. Sculpted multilayers were also found in tiger beetles [9] and butterflies [12]. The elytral surface morphology due to the sculpted multilayer can produce the following optical effects.

For a flat multilayer, its peak reflectance is rather high, leading to bright structural coloration, which can be found in many beetles [6,7]. In beetles *Chlorophila obscuripennis*, the elytral surface comprises an array of hexagonal pits. As a result, the effective area for specular reflection is much smaller than that of a flat multilayer, leading to an inconspicuous structural bluish green color. The adoption of this inconspicuous bluish green color is more advantageous for camouflage against green backgrounds, especially on diffuse leafy surfaces.

The average thickness of bilayer in the sculpted multilayer is different in different regions, leading to different structural coloration: the ridges appear green and the basins display a cyan color. However, these individual colors cannot be resolved by the naked eye. As a result, we can only perceive a mixed bluish green color. Such spatial color mixing has been reported in tiger beetles [9] and butterflies [12], and it is also used in color television, printing, and pointillistic painting.

Another important feature of the sculpted multilayer is the inclined sides of pits. For a flat multilayer, only specular reflection can occur. For a sculpted multilayer, however, both specular and nonspecular reflections can be expected. Interestingly, nonspecular reflection, produced by the inclined sides, can give rise to light emergence at directions that differ from the reflected angle. Consequently, structural color can be perceived in a much wider range of viewing angles. This feature may be of significance in signal communications and conspecific recognition.

In the wing scales of the Indonesian male *Papilio palinurus* butterfly [12], their surface comprises a regular array of squarelike pits. The sculpted multilayer was found to produce a yellow color at the basins and a blue color at the inclined sides, causing a mixed green color. In beetles *Chlorophila obscuripennis*, however, the inclined sides produce a dull blue which gives a minor contribution to color mixing. The production of a blue color at the inclined sides in *Papilio palinurus* butterfly lies in double reflection by a pair of orthogonal surfaces inclined about 45° to the scale surface. At normal incidence, reflected light from one inclined surface is directed across to its adjacent inclined side, where it is reflected back to the incident direction. In beetles *Chlorophila obscuripennis*, the inclined angle is, however, much smaller than 45°. Moreover, the pits have a hexagonal profile. At normal incidence, double reflection cannot cause light emergence back to the incidence direction. However, at oblique incidence, we can still observe a dull structural color produced by the inclined sides. This can be seen from Fig. 1 where the inclined sides display a dull blue color due to the fact that incidence is not exactly normal in optical microscope observations.

## ACKNOWLEDGMENTS

This work was mostly supported by the 973 Program. Partial support from NSFC, PCSIRT, and the Shanghai Science and Technology Commission is also acknowledged.

[1] M. F. Land, Prog. Biophys. Mol. Biol. **24**, 75 (1972).
[2] D. L. Fox, *Animal Biochromes and Structural Colors* (University of California Press, Berkeley, CA, 1976).
[3] M. Srinivasarao, Chem. Rev. (Washington, D.C.) **99**, 1935 (1999).
[4] A. R. Parker, J. Opt. A, Pure Appl. Opt. **2**, R15 (2000).
[5] P. Vukusic and J. R. Sambles, Nature (London) **424**, 852 (2003).
[6] S. Kinoshita and S. Yoshioka, ChemPhysChem **6**, 1442 (2005).
[7] A. R. Parker, J. R. Soc., Interface **2**, 1 (2005).
[8] C. W. Mason, J. Phys. Chem. **31**, 321 (1927); **31**, 1856 (1927).
[9] T. D. Schultz and M. A. Rankin, J. Exp. Biol. **117**, 87 (1985); T. D. Schultz and G. D. Bernard, Nature (London) **337**, 72 (1989).
[10] A. R. Parker, D. R. Mckenzie, and M. C. J. Large, J. Exp. Biol. **201**, 1307 (1998).
[11] P. Vukusic, J. R. Sambles, C. R. Lawrence, and R. J. Wootton, Proc. R. Soc. London, Ser. B **266**, 1402 (1999).
[12] P. Vukusic, J. R. Sambles, and C. R. Lawrence, Nature (London) **404**, 457 (2000).
[13] B. Gralak, G. Tayeb, and S. Enoch, Opt. Express **9**, 567 (2001).
[14] P. Vukusic, J. R. Sambles, C. R. Lawrence, and R. J. Wootton, Proc. R. Soc. London, Ser. B **269**, 7 (2002).
[15] A. R. Parker, V. L. Welch, D. Driver, and N. Martini, Nature (London) **426**, 786 (2003).
[16] J. P. Vigneron, J.-F. Colomer, N. Vigneron, and V. Lousse, Phys. Rev. E **72**, 061904 (2005).
[17] C. W. Mason, J. Phys. Chem. **27**, 201 (1923).
[18] C. H. Greenwalt, W. Brandt, and D. D. Friel, J. Opt. Soc. Am. **50**, 1005 (1960).
[19] J. Dyck, Biol. Skr. (Copenhagen) **18**, 1 (1971); Z. Zellforsch Mikrosk Anat. **115**, 17 (1971); Biol. Skr. (Copenhagen) **30**, 2 (1987).
[20] H. Durrer, in *Biology of the Integument. 2. Vertebrates*, edited by J. Bereiter-Hahn, A. G. Matoltsky, and K. S. Richards (Springer, Berlin, 1986), p. 239.
[21] R. O. Prum, R. Torres, S. Williamson, and J. Dyck, Nature (London) **396**, 28 (1998); R. O. Prum, R. H. Torres, S. Williamson, and J. Dyck, Proc. R. Soc. London, Ser. B **266**, 13 (1999).
[22] D. Osorio and A. D. Ham, J. Exp. Biol. **205**, 2017 (2002).
[23] M. D. Shawkey, A. M. Estes, L. M. Siefferman, and G. E. Hill, Proc. R. Soc. London, Ser. B **270**, 1455 (2003).
[24] J. Zi, X. Yu, L. Li, X. Hu, C. Xu, X. Wang, X. Liu, and R. Fu, Proc. Natl. Acad. Sci. U.S.A. **100**, 12576 (2003); Y. Li, Z. Lu, H. Yin, X. Yu, X. Liu, and J. Zi, Phys. Rev. E **72**, 010902(R) (2005).
[25] H. Yin, L. Shi, J. Sha, Y. Li, Y. Qin, B. Dong, S. Meyer, X. Liu, L. Zhao, and J. Zi, Phys. Rev. E **74**, 051916 (2006).
[26] J. P. Vigneron, J.-F. Colomer, M. Rassart, A. L. Ingram, and V. Lousse, Phys. Rev. E **73**, 021914 (2006).
[27] J. N. Lythgoe and J. Shand, J. Exp. Biol. **141**, 313 (1989).
[28] A. R. Parker, R. C. McPhedran, D. R. Mckenzie, L. C. Botten, and N.-A. P. Nicorovici, Nature (London) **409**, 36 (2001).
[29] V. Welch, J. P. Vigneron, V. Lousse, and A. Parker, Phys. Rev. E **73**, 041916 (2006).
[30] D. W. Lee and J. B. Lowry, Nature (London) **254**, 50 (1975).
[31] D. W. Lee, Nature (London) **349**, 260 (1991).
[32] R. M. Graham, D. W. Lee, and K. Norstog, Am. J. Bot. **80**, 198 (1993).
[33] J. P. Vigneron, M. Rassart, Z. Vértesy, K. Kertész, M. Sarrazin, L. P. Biró, D. Ertz, and V. Lousse, Phys. Rev. E **71**, 011906 (2005).
[34] A. R. Parker, Mater. Today **5**, 26 (2002).
[35] M. Born and E. Wolf, *Principles of Optics* (Cambridge University Press, Cambridge, 1999).